

Update for E12-07-104: Measurement of the Neutron Magnetic Form Factor at High Q^2 Using the Ratio Method on Deuterium

G.P. Gilfoyle^{*†}, *W.K. Brooks*^{*}, and *K. Hafidi*^{*} for the CLAS Collaboration

1 Introduction

In JLab Experiment E12-07-104 we intend to dramatically extend the reach of our understanding of a fundamental feature of the neutron; its magnetic form factor G_M^n . The elastic electromagnetic form factors (EEFFs) describe the distribution of charge and magnetization inside the nucleon at low Q^2 and probe the quark structure at higher Q^2 . This experiment is part of a broad program at JLab to measure the EEFFs, map the internal landscape of the nucleon, and test non-perturbative Quantum Chromodynamics (QCD) and QCD-inspired models of the nucleon (see NSAC Long-Range Plan [1]). The measurement will cover the range $Q^2 = 3.5 - 14.0 \text{ GeV}^2$ with systematic uncertainties less than 3%. Statistical uncertainties will be about 3% in the highest Q^2 bin in this range and significantly less at lower Q^2 . The anticipated range and systematic uncertainties of the experiment are shown in Figure 1. The reduced magnetic form factor $G_M^n/(\mu_n G_D)$ is plotted versus Q^2 where μ_n is the neutron magnetic moment and $G_D = 1/(1 + Q^2/\Lambda^2)^2$ is the dipole form factor with $\Lambda^2 = 0.71 \text{ GeV}^2$. We used the recent parameterization of the world's data on G_M^n in Ref [10] to predict the reduced form factor. Also shown are selected world's data for G_M^n including

*Co-spokesperson

†Contact person

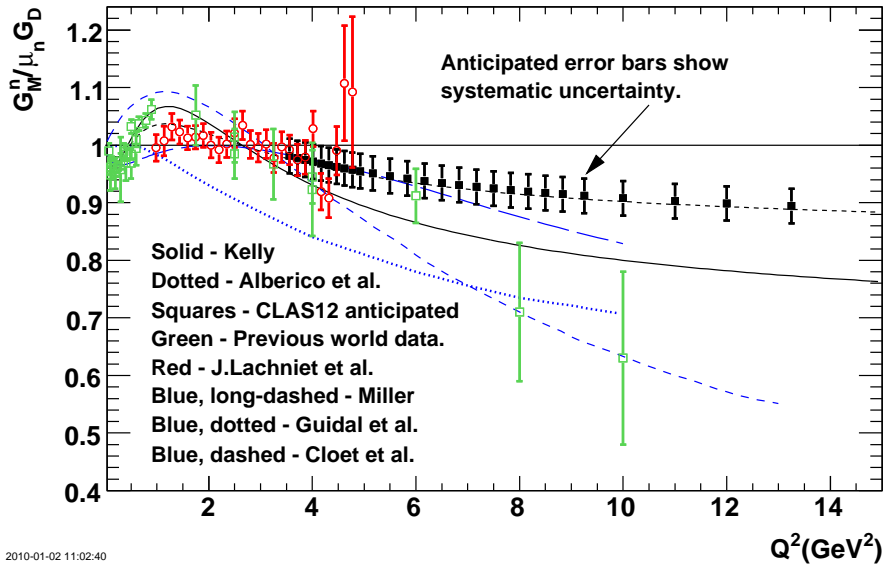


Figure 1: Selected data [2, 3, 4, 5, 6, 7, 8, 9] and anticipated results for G_M^n for 56 days of running with CLAS12 (black, filled squares) in units of $\mu_n G_D$ as a function of Q^2 . The anticipated CLAS12 results follow a fit to the world data on G_M^n that includes the recent CLAS6 G_M^n results [10]. The red, open circles are the CLAS6 results. Other curves are described in the text.

the recent CLAS6 results (red, open circles)[2]. The proposed CLAS12 experiment (black, closed squares) will nearly triple the upper limit of the previous CLAS6 measurement and provide precise data well past any existing measurement. Other aspects of Figure 1 are discussed below.

To measure G_M^n we will use the ratio of quasielastic $e - n$ to quasielastic $e - p$ scattering on deuterium. The ratio method is less vulnerable to systematic uncertainties than previous methods and we will have consistency checks between different detector components of CLAS12 and an overlap with our previous CLAS6 measurements. A liquid-hydrogen/liquid-deuterium, dual target will be used to make *in situ* measurements of the neutron and proton detection efficiencies. We take advantage of the large acceptance of CLAS12 and veto events with additional particles (beyond $e - n$ and $e - p$ coincidences) to reduce the inelastic background. We expect to limit the systematic uncertainties to 3% or less [11]. This experiment can be done with the base equipment for CLAS12 and was approved by PAC32.

This experiment is part of a series to measure the elastic, electromagnetic form factors of the nucleon at JLab [11, 12, 13, 14, 15, 16]. The PAC has approved experiments in all three halls to measure the four EEFs. That set includes E12-09-019 to measure G_M^n in Hall A over the same Q^2 as our experiment. Making both measurements will ‘allow a better control of the systematic error on G_M^n ’ (see PAC 34 report [17]). In this update we discuss recent, relevant measurements emphasizing developments in the last two years since E12-07-104 was approved. We also present new theoretical developments and analyses and connect this experiment with the Hall A one.

2 Experimental Status

New experimental results have been produced since PAC32. The CLAS6 measurement of the neutron magnetic form factor has been published [2]. The results are shown as the red points in Figure 2 and compared with several theoretical models and selected world data. The CLAS6 data are surprisingly consistent with the dipole parameterization. This was unexpected because previous measurements show the reduced G_M^n decreasing at larger Q^2 although with large uncertainties ($G_M^n/\mu_n G_D = 0.62 \pm 0.15$ at $Q^2 = 10 \text{ GeV}^2$ [9]); see the green points in Figure 1 for $Q^2 \geq 4.0 \text{ GeV}^2$.

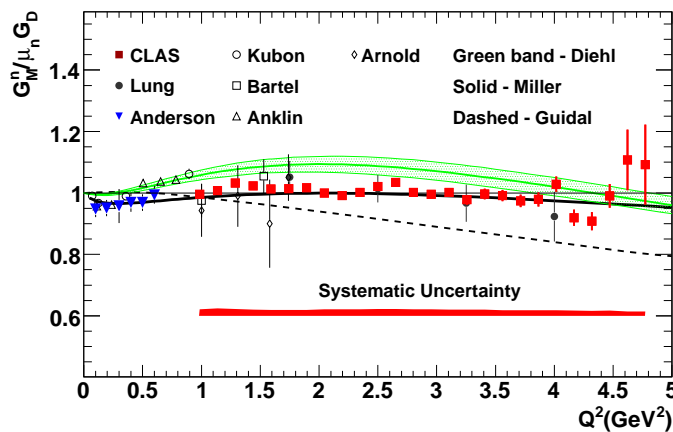


Figure 2: Results for $G_M^n/(\mu_n G_D)$ from the CLAS6 measurement are compared with a selection of previous data [3, 4, 5, 6, 7, 8] and theoretical calculations [18, 19, 20].

The solid, black curve in Figure 1 shows a fit by Kelly [21] to the world data without the CLAS6 results, reflecting this drop with Q^2 . The dashed curve from Alberico *et al.* [10] is a fit that includes the CLAS6 results which falls more slowly with Q^2 . The other curves shown in Figure 2 are from Diehl *et al.* [18], Guidal *et al.* [19], and Miller [20] and are all constrained by the world's previous data without the CLAS6 results. The curves from Refs. [18] and [19] use generalized parton distributions (GPDs) to characterize the EEFs at low Q^2 and then extend their calculations to higher Q^2 . Both fail to reproduce the CLAS6 data. In Miller's calculation the nucleon is treated using light-front dynamics as a relativistic system of three bound quarks and a surrounding pion cloud (solid curve in Figure 2). The model gives a good description of much of the previous data (including the other three EEFs) even at high Q^2 and is consistent with the CLAS6 results.

Recent measurements [22] and planned ones [12, 13, 14, 15, 16] will reduce the systematic uncertainties on the proposed G_M^n measurement. Extracting G_M^n depends on precise knowledge of the proton cross section and the neutron electric form factor G_E^n . The neutron electric form factor is known to be small in this Q^2 range and contributes at most about 0.7% to the anticipated systematic uncertainty [11]. Recent measurements of the ratio G_E^n/G_M^n [22] will improve our knowledge of this quantity and drive down the uncertainty on its contribution. The proton cross section is well known in this Q^2 region and contributes at most about 1.5% to the anticipated systematic uncertainty [11]. We expect this contribution to decline in the future because there is a planned 12 GeV experiment to precisely measure this quantity [13].

The broad effort at JLab to measure all four of the elastic electromagnetic form factors is in a Q^2 region with significant discovery potential. All the EEFs are needed to untangle nucleon structure [23]. For example, measuring the ratio of the proton electric to magnetic form factor G_E^p/G_M^p using polarization observables revealed a striking difference from earlier measurements [24]. Instead of being constant as expected this ratio fell linearly and appeared to be headed for a zero crossing at $Q^2 \approx 8 \text{ GeV}^2$. This has sparked a revival of interest in these form factors and dramatically changed our picture of the proton. Recent, preliminary results from the GEp(III) collaboration for G_E^p/G_M^p using the recoil polarization method show a decrease with Q^2 , but with a shallower slope [25]. The ratio G_E^n/G_M^n was recently measured with greater precision and at higher Q^2 than ever before [25]. Those researchers used the recent CLAS6 measurement of G_M^n to extract G_E^n . The preliminary results for the points at Q^2 of 2.5 GeV^2 and 3.5 GeV^2 are 2-4 standard deviations away from the Galster parameterization; suggesting the onset of changes from the lower Q^2 behavior. All of these new, intriguing results are in the same Q^2 range as the proposed CLAS12 G_M^n measurement.

3 Theoretical Status

Progress has been made on the theory side of our understanding of the EEFs. Mapping the internal geography of the neutron is a central goal of the 12 GeV Upgrade [1]. The interpretation of the form factors in non-relativistic kinematics has long been in terms of the charge and magnetization densities of the nucleons with a positive, central core in the neutron and a negative region on its periphery. For the relativistic case where $Q^2 > M_N^2$ this simple interpretation becomes model dependent. Switching to the infinite momentum frame allows one to escape this model dependence, but apparently contradicts the traditional view [26]. Miller and Arrington [27] use a GPD model to resolve this issue; demonstrating the importance of GPDs to understanding nucleon structure.

Another central goal of the 12 GeV Upgrade is to understand non-perturbative QCD and QCD-inspired models. Cloët *et al.* employ dynamically dressed quarks using the Dyson-Schwinger Equations in a framework that is fully Poincaré covariant and symmetry preserving; an essential feature as we explore higher Q^2 [28]. The degrees of freedom in this model are the three, dressed

quarks and nonpointlike quark-quark (diquark) correlations. The only free parameter in the model is the diquark radius. Figure 3 shows the ratio of the neutron electric to magnetic form factors for two different values of the diquark radius (solid curve and long-dashed curve), data from Madey *et al.* [29], and the Kelly parameterization (dashed curve) [21]. The Cloët *et al.* prediction diverges

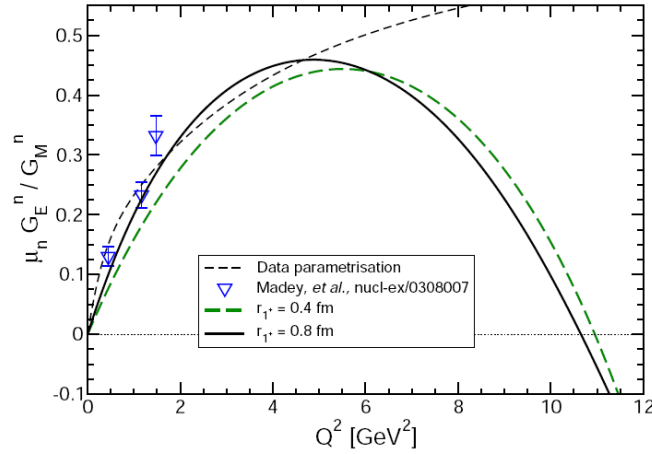


Figure 3: Result for the normalized ratio of Sachs electric and magnetic form factors for the neutron computed with two different diquark radii. Short-dashed curve: parameterization of Ref. [21]. Down triangles: data from Ref. [29].

dramatically from the data parameterization at $Q^2 \approx 5 \text{ GeV}^2$ and then bends over and crosses zero at $Q^2 \approx 11 \text{ GeV}^2$. This behavior marks this region of Q^2 as one of potential discovery value and lies well within the Q^2 of our proposed experiment. To study this region further we show some representative calculations in Figure 1. The blue curves are from Miller and Guidal *et al.*, (described in Section 2) and extended to higher Q^2 and Cloët *et al.* All three curves differ measurably in magnitude and/or slope somewhere in the range $Q^2 = 6 - 14 \text{ GeV}^2$. There is an opportunity here to distinguish among competing pictures of the neutron. We note here the uncertainties on the anticipated CLAS12 data are systematic ones. We expect the statistical ones to be about the same size (3%) in the highest bin and much smaller at lower Q^2 .

We also want to touch on truly *ab initio* calculations performed using lattice QCD. These calculations are still limited in reach to $Q^2 \approx 1 \text{ GeV}^2$, but we expect that significant progress will be made by the time the proposed experiment is complete. This is where the broad assault on the EEFs at JLab is essential. The EEFs can be formed into isovector and isoscalar combinations that are sensitive to different physical effects. The isovector combination is free of disconnected contributions which are notoriously difficult to compute on the lattice. This freedom will make the isovector form factor an early test of lattice QCD as the calculations reach higher Q^2 .

4 Experimental Method and Relationship To Existing Experiments

We now outline the experimental technique and compare the CLAS12 procedures with others. More details are in Ref. [11]. We propose to use the ratio of quasielastic $e - n$ to $e - p$ scattering from a deuterium target to measure G_M^n in the range $Q^2 = 3.5 - 14.0 \text{ GeV}^2$. This technique

significantly reduces uncertainties associated with other methods and has been used by us [2] and others [6, 30, 31, 32, 33] to measure G_M^n (see Figure 2). The method is based on the ratio

$$R = \frac{\frac{d\sigma}{d\Omega}(^2\text{H}(e, e'n)_{QE})}{\frac{d\sigma}{d\Omega}(^2\text{H}(e, e'p)_{QE})} = a(Q^2) \frac{\sigma_{mott}^n (G_E^n{}^2 + \frac{\tau_n}{\epsilon_n} G_M^n{}^2) \left(\frac{1}{1+\tau_n} \right)}{\frac{d\sigma}{d\Omega}(^1\text{H}(e, e')p)} \quad (1)$$

for quasielastic (QE) kinematics. The right-hand side is written in terms of the free nucleon form factors and where $\tau = Q^2/4M^2$ and $\epsilon = 1/[1 + 2(1 + \tau) \tan^2(\theta/2)]$. Deviations from this ‘free ratio’ assumption are parameterized by the factor $a(Q^2)$ which can be calculated from deuteron models and is close to unity at large Q^2 . The results of other measurements of the proton cross section and the neutron electric form factor are used to extract G_M^n . The ratio R is insensitive to the luminosity, electron acceptance, electron reconstruction efficiency, trigger efficiency, the deuteron wave function used in $a(Q^2)$, and radiative corrections [2, 34]. In the Hall A G_M^n experiment (E12-09-019), the ratio method is also used.

An essential step in applying the ratio method is selecting quasielastic (QE) events and reducing the inelastic background. The selection criteria should be the same for $e - p$ and $e - n$ events (to avoid biasing the results) and we want to take advantage of the angular precision of CLAS12. Quasielastic neutron and proton events are chosen by applying a cut on θ_{pq} , the angle between the nucleon 3-momentum and the momentum transfer \vec{q} . Inelastic events tend to be emitted at large θ_{pq} while QE events are emitted along the direction of \vec{q} . Next, we select events with $W^2 = M_N^2$. In this Q^2 regime, the width of the residual mass spectrum W^2 becomes large so that contamination of the QE peak with inelastic events is a greater problem than at lower Q^2 . Figure 4 shows this kinematical effect and the impact of requiring $\theta_{pq} < 1.5^\circ$ on the W^2 spectrum for $Q^2 = 12.5 - 14.0 \text{ GeV}^2$. The left-hand panel shows the results of a simulation of the reaction described in the original proposal [11] for $e - n$ coincidences at a beam energy of 11 GeV and in the highest Q^2 bin ($Q^2 = 12.5 - 14.0 \text{ GeV}^2$) where we expect to have statistical precision equal to the anticipated systematic uncertainty of 3%. The red histogram shows the contribution of the QE events, the green one shows the inelastic events, and the black one is the total. The QE events are overwhelmed by the inelastic background in the left-hand panel. Requiring $\theta_{pq} < 1.5^\circ$ for the

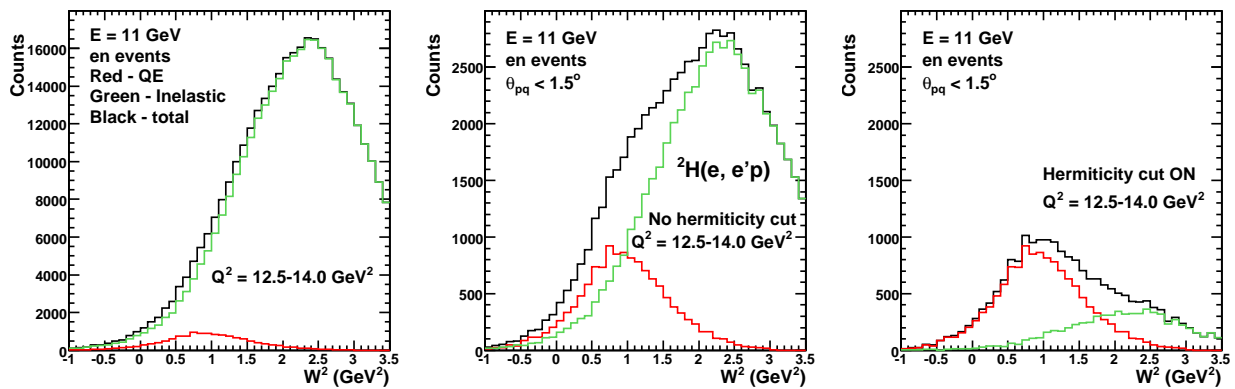


Figure 4: The impact of the hermiticity cut is shown. The left-hand panel displays the W^2 spectra for simulated $e - n$ events. In the middle panel, the neutrons are required to have $\theta_{pq} < 1.5^\circ$. In the right-hand panel, we add the hermiticity cut. The number of events shown is not representative of the anticipated value.

neutron (middle panel) considerably reduces the inelastic background. Nevertheless, the QE events are still a shoulder on a larger inelastic peak. We now take full advantage of the large acceptance of CLAS12. The inelastic events that emit nucleons and contaminate the QE spectrum have other, associated particles (pions, photons, *etc.*). CLAS12 will detect many of those associated particles. In the right-hand panel we have applied a multiparticle veto or hermiticity cut. Electron-proton events that have a third particle and come from inelastic events (and are part of event sample in the other two panels) are rejected. This reduces the inelastic background by about a factor of 4-5 here; the quasielastic peak now clearly rises out of the inelastic noise. We can then apply a cut on W^2 to remove additional inelastic events. In the example shown, the contribution of the background in the region of the QE peak for $W^2 < 1.2 \text{ GeV}^2$ drops from 45% of the total in the middle panel to 11% in the right-hand panel after applying the hermiticity cut. Notice also there is no effect on the events in QE peak (red histogram going from the middle panel to the right-hand one). We want to emphasize here that Figure 4 represents a worst case scenario. We simulated the reaction for the highest Q^2 bin (12.5 – 14.0 GeV^2) where we expect to obtain statistical uncertainty that is equal to or less than our expected systematic uncertainty of 3%. The data at lower Q^2 will have less kinematic spreading and inelastic contamination. See the E12-07-104 proposal for the results of a simulation in the middle of the Q^2 range of the proposed experiment [11]. The approved experiment in Hall A to measure G_M^n (E12-09-019) does not have a multiparticle veto. In that experiment the angular resolution and high luminosity of the Hall A spectrometers enables one to place restrictive cuts on θ_{pq} to isolate the QE events.

The G_M^n measurement in CLAS12 has important consistency checks. Neutrons will be measured in two subsystems of the forward detector. One of those subsystems, the forward calorimeter (FC), consists of the electromagnetic calorimeter (EC) used in CLAS6 (and the CLAS6 G_M^n measurement) and a new, pre-shower calorimeter (PCAL) which is located in front and covers the face of the EC. The forward time-of-flight (TOF) system will consist of the same detectors used in CLAS6 (thickness 25 mm) along with two new layers of scintillators (one is the same thickness and the other is thicker at 30 mm). These two subsystems will enable us to make semi-independent measurements of the $e - n$ production in CLAS12 and provide a vital cross check on the measurement. The approved experiment in Hall A to measure G_M^n (E12-09-019) does not have an internal consistency check like this one. The CLAS6 measurement will also have a large overlap ($Q^2 = 3.5 - 4.8 \text{ GeV}^2$) with the previous CLAS6 G_M^n measurement (see Figure 1). Since we are reusing some of the same detector subsystems that were used in the CLAS6 G_M^n experiment (the EC and one of the forward TOF panels) this will provide another consistency check on our CLAS12 results.

An essential aspect of the neutron measurement in the TOF and FC systems is measuring the neutron detection efficiency. We will use the $p(e, e' \pi^+ n)$ reaction as a source of tagged neutrons. Electrons and π^+ 's will be detected in CLAS12 and missing mass used to select candidate neutrons (found events). We then predict the position of the neutron in CLAS12 and search for it (if a neutron is found we call these reconstructed events). The ratio of reconstructed to found events gives us the detection efficiency. This will be done in CLAS12 with a unique, dual target. Co-linear, liquid hydrogen and deuterium cells will provide production and calibration events simultaneously and under the same conditions (*in situ*). This reduces our vulnerability to variations in detector gains, beam properties, *etc.* The PAC32 report described this method as ‘elegant.’ In the Hall A G_M^n experiment (E12-09-019), a radiator and a hydrogen target will be placed periodically in the beam so the $p(\gamma, \pi^+)n$ reaction can be used to provide tagged neutrons [14].

In the CLAS6 measurement we used the same techniques described here to measure the neutron production and detection efficiency. To demonstrate the power of these methods we show Figure 5 from Ref [2]. It shows G_M^n measured simultaneously with the CLAS6 TOF and EC subsystems (that will be reused in CLAS12). Two beam energies were used in the CLAS6 measurement so there are

four semi-independent data sets. The uncertainties are statistical ones only. The four measurements are consistent within the statistical uncertainties, suggesting the systematic uncertainties are well-controlled and small. Any overall differences are within the 2-3% systematic uncertainty of the CLAS6 G_M^n experiment. In CLAS12 we will have similar internal consistency checks to validate our results for G_M^n and the systematic uncertainty.

In Figure 6 we show the anticipated number of neutron and proton events as a function of Q^2 (red and blue points and left-hand scale) and the uncertainty on G_M^n (right-hand scale). Instead of using the dipole approximation as we did in the original E12-07-104 proposal the cross sections for proton

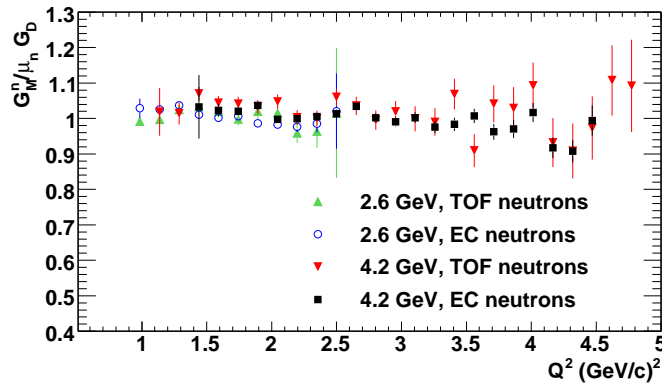


Figure 5: Comparison of G_M^n measured with different CLAS6 subsystems (TOF and EC) and for two different beam energies [2].

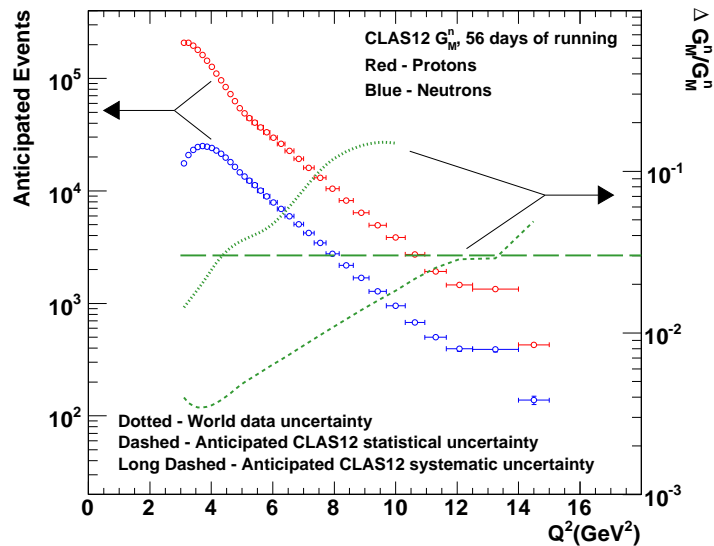


Figure 6: Run statistics for the CLAS12 G_M^n experiment (E12-07-104) for 56 days of running. Proton cross sections were obtained using the Kelly fit [21]. Neutron cross sections were obtained using the Galster fit for G_E^n and the Alberico *et al.* [10] fit for G_M^n . The green, dotted line is the current uncertainty on G_M^n for the world data, the green, short-dashed line is our anticipated statistical uncertainty, and the green, long-dashed line is our goal of 3% systematic uncertainty.

events were calculated using the fits from Kelly [21] for the proton form factors. For the neutron cross sections the Galster fit was used for G_E^n , and the Alberico *et al.* fit for G_M^n [10] that includes the recent CLAS6 G_M^n data. We also included the effect of a cut requiring $W^2 < 1.2 \text{ GeV}^2$. Bin sizes in the low Q^2 region where we overlap with the CLAS6 measurement match the CLAS6 ones and then increase gradually. The bin for the range $Q^2 = 12.5 - 14 \text{ GeV}^2$ will have statistical precision equal to the anticipated systematic uncertainty of 3%. Depending on the target position we can reach as far as $Q^2 = 15 \text{ GeV}^2$, but with diminished statistical precision. This value of Q^2 corresponds to the largest electron scattering angle we will measure in the forward detector in CLAS12. At lower Q^2 the statistical precision increases rapidly. Over the range $Q^2 = 3.5 - 14.0 \text{ GeV}^2$ we have statistical uncertainties at or below 3% (our goal for the upper limit on the systematic uncertainty) and typically much lower (green, dashed line in Figure 6). These uncertainties are far below the current precision on G_M^n (green, dotted line). The Hall A measurement (E12-09-119) will have better statistical precision across the full Q^2 range ($3.5 - 14.0 \text{ GeV}^2$) than the CLAS12 one. Both experiments will be limited by systematic uncertainties.

We have set a goal of 3% as the upper limit on the systematic uncertainty (long-dashed line in Figure 6). Based on our CLAS6 experience, the largest contributors to the systematic uncertainty will be the parameterization of the neutron detection efficiency (NDE) for the TOF and EC systems, the uncertainty on the proton cross section, and the uncertainty on G_E^n . We estimated those contributions to have maximum values of 0.75% (NDE parameterization), 1.2% (proton cross section), and 1.4% (G_E^n) (see Section 3.5 of Ref [11]). The uncertainties on the proton cross section and G_E^n are lower over most of the Q^2 range and will shrink with future measurements. We also estimated the systematic uncertainty due to the inelastic background subtraction using the highest Q^2 bin with good statistics ($12.5 - 14.0 \text{ GeV}^2$) again as a worst-case scenario. In this bin 11% of the neutron events and 12% of the proton events in the range $W^2 < 1.2 \text{ GeV}^2$ are inelastic background. We expect to determine that value within 20%; giving us a systematic uncertainty of 2% in the ratio R and 1% in G_M^n . We added all these contributions in quadrature including weighting the effect of the TOF NDE measurement less (because the TOF efficiency is about one-sixth of the EC efficiency). We obtain an estimate of the maximum anticipated systematic uncertainty of 2.4%; this result determined our goal of 3% for the systematic uncertainty. In the Hall A experiment (E12-09-119) the anticipated systematic uncertainties on G_M^n are in the range of 1.2%-2.9%

We also note here that like CLAS6, CLAS12 will have an electron trigger so a wide range of data will be collected. Experiments with different physics requirements can use the same data set. The CLAS12 experiment will make efficient use of beam time by allowing other experiments to run concurrently with E12-07-104. Experiments E12-09-007 and E12-09-008 will study nucleon structure using semi-inclusive deep inelastic scattering. They have been approved and will run concurrently with us [35, 36].

To summarize, the scientific motivation for measuring the neutron magnetic form factor is more compelling than when E12-07-104 was approved. The dipole form of G_M^n has returned to prominence for $Q^2 = 1.0 - 4.5 \text{ GeV}^2$. At higher Q^2 ($5 - 13 \text{ GeV}^2$) we have observed new, surprising behavior in the other form factors (a possible zero crossing in G_E^p/G_M^p), developed QCD-inspired models that diverge widely, and predictions for a zero crossing in G_E^n . To explore this new territory JLab will measure all of the EEFs. The CLAS12 experiment will use a tested method for measuring G_M^n and push the frontier of our understanding of the neutron magnetic form factor up to $Q^2 = 14 \text{ GeV}^2$ and with high precision. The ability to veto multiparticle final states dramatically reduces the background from inelastic events that contaminate the QE peak. We will use a dual-cell target for precise, *in situ* measurements of the neutron detection efficiency as demonstrated in the CLAS6 experiment. Finally, with CLAS12 we have several important consistency checks using different detector subsystems of CLAS12 (TOF and EC) to validate our results.

References

- [1] Nuclear Science Advisory Committee. *The Frontiers of Nuclear Science*. US Department of Energy, 2007.
- [2] J. Lachniet, A. Afanasev, H. Arenhövel, W. K. Brooks, G. P. Gilfoyle, D. Higinbotham, S. Jeschonnek, B. Quinn, M. F. Vineyard, et al. Precise Measurement of the Neutron Magnetic Form Factor G_M^n in the Few-GeV² Region. *Phys. Rev. Lett.*, 102(19):192001, 2009.
- [3] W. Bartel et al. *Nucl. Phys. B*, 58:429, 1973.
- [4] G. Kubon et al. *Phys. Lett. B*, 524:26–32, 2002.
- [5] A. Lung et al. *Phys. Rev. Lett.*, 70(6):718–721, Feb 1993.
- [6] H. Anklin et al. *Phys. Lett. B*, 428:248–253, 1998.
- [7] B. Anderson et al. *Phys. Rev. C*, 75:034003, 2007.
- [8] R. G. Arnold et al. Measurements of transverse quasielastic electron scattering from the deuteron at high momentum transfers. *Phys. Rev. Lett.*, 61(7):806–809, Aug 1988.
- [9] S. Rock et al. Measurement of Elastic Electron-Neutron Cross Sections up to $Q^2 = 10$ (GeV/c)². *Phys. Rev. Lett.*, 49(16):1139–1142, Oct 1982.
- [10] W. M. Alberico, S. M. Bilenky, C. Giunti, and K. M. Graczyk. Electromagnetic form factors of the nucleon: New fit and analysis of uncertainties. *Phys. Rev. C (Nuclear Physics)*, 79(6):065204, 2009.
- [11] G.P. Gilfoyle, W.K. Brooks, S. Stepanyan, M.F. Vineyard, S.E. Kuhn, J.D. Lachniet, L.B. Weinstein, K. Hafidi, J. Arrington, R. Geesaman, D. Holt, D. Potterveld, P.E. Reimer, P. Solvignon, M. Holtrop, M. Garcon, S. Jeschonnek, and P. Kroll. Measurement of the Neutron Magnetic Form Factor at High Q^2 Using the Ratio Method on Deuterium. E12-07-104, Jefferson Lab, Newport News, VA, 2007.
- [12] E.J. Brash, M.K. Jones, Punjabi V., et al. G_E^p/G_M^p with an 11 GeV electron beam. E12-09-001, Jefferson Lab, Newport News, VA, 2009.
- [13] S. Gilad et al. Precision Measurement of the Proton Elastic Cross Section at High Q^2 . E12-07-108, Jefferson Lab, Newport News, VA, 2007.
- [14] B. Quinn, B. Wojtsekhowski, R. Gilman, et al. Precision Measurement of the Neutron Magnetic Form Factor up to $Q^2 = 18.0$ (GeV/c)² by the Ratio Method. E12-09-119, Jefferson Lab, Newport News, VA, 2009.
- [15] B.D. Anderson, J. Arrington, S. Kowalski, R. Madey, B. Plaster, A.Yu. Semenov, et al. The Neutron Electric Form Factor at Q^2 up to 7 (GeV/c)² from the Reaction ${}^2H(e, e'n){}^1H$ via Recoil Polarimetry. E12-09-006, Jefferson Lab, Newport News, VA, 2009.
- [16] B. Wojtsekhowski et al. Measurement of the Neutron Electromagnetic Form Factor Ratio G_E^n/G_M^n at High Q^2 . E12-09-016, Jefferson Lab, Newport News, VA, 2009.
- [17] JLab Physics Advisory Committee. PAC34 Report. Technical report, Jefferson Laboratory, 2009.

- [18] M. Diehl et al. *Eur. Phys. J. C*, 39:1, 2005.
- [19] M. Guidal et al. *Phys. Rev. D*, 72:054013, 2005.
- [20] G.A. Miller. *Phys. Rev. C*, 66:032201, 2002.
- [21] J. J. Kelly. Simple parametrization of nucleon form factors. *Phys. Rev. C*, 70(6):068202, Dec 2004.
- [22] Seamus Riordan. Measurements of the electric form factor of the neutron at high momentum transfer. *AIP Conf. Proc.*, 1149:615–618, 2009.
- [23] M. Diehl, Th. Feldmann, R. Jakob, and P. Kroll. *Eur. Phys. J. C*, 39:1, 2005.
- [24] M. K. Jones et al. G_E^p/G_M^p Ratio by Polarization Transfer in $\vec{e}p \rightarrow e\vec{p}$. *Phys. Rev. Lett.*, 84(7):1398–1402, Feb 2000.
- [25] Kees de Jager. The Super Bigbite Project: a Study of Nucleon Form Factors. 2009.
- [26] Gerald A. Miller. Charge densities of the neutron and proton. *Phys. Rev. Lett.*, 99(11):112001, 2007.
- [27] Gerald A. Miller and John Arrington. The neutron negative central charge density: an inclusive- exclusive connection. *Phys. Rev.*, C78:032201, 2008.
- [28] I. C. Cloet, G. Eichmann, B. El-Bennich, T. Klahn, and C. D. Roberts. Survey of nucleon electromagnetic form factors. *Few Body Syst.*, 46:1–36, 2009.
- [29] R. Madey et al. *Phys. Rev. Lett.*, 91:122002, 2003.
- [30] C.E. Hyde-Wright and K.deJager. Electromagnetic Form Factors of the Nucleon and Compton Scattering. *Ann. Rev. Nucl. Part. Sci.*, 54.
- [31] H. Anklin et al. *Phys. Lett. B*, 336:313–318, 1994.
- [32] G. Kubon et al. *Phys. Lett. B*, 524:26–32, 2002.
- [33] E. E. W. Bruins et al. Measurement of the neutron magnetic form factor. *Phys. Rev. Lett.*, 75(1):21–24, Jul 1995.
- [34] J.D. Lachniet, W.K. Brooks, G.P. Gilfoyle, B. Quinn, and M.F. Vineyard. A high precision measurement of the neutron magnetic form factor using the CLAS detector. CLAS Analysis Note 2008-103, Jefferson Lab, 2008.
- [35] K. Hafidi et al. Studies of partonic distributions using semi-inclusive production of Kaons. E12-09-007, Jefferson Lab, Newport News, VA, 2009.
- [36] K. Hafidi et al. Study of the Boers-Mulders Asymmetry in Kaon Electroproduction with Hydrogen and Deuterium Targets. E12-09-008, Jefferson Lab, Newport News, VA, 2009.